

Interaction–Deletion: A Composite Energy Method for the Optimization of Molecular Systems Selectively Removing Specific Nonbonded Interactions

Published as part of *The Journal of Physical Chemistry* virtual special issue “125 Years of *The Journal of Physical Chemistry*”.

Ankur K. Gupta, Benjamin C. Gamoke, and Krishnan Raghavachari*



Cite This: *J. Phys. Chem. A* 2021, 125, 4668–4682



Read Online

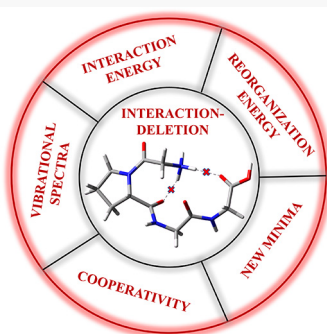
ACCESS |

Metrics & More

Article Recommendations

Supporting Information

ABSTRACT: The complex interactions between different portions of a large molecule can be challenging to analyze through traditional electronic structure calculations. Moreover, standard methods cannot easily quantify the physical consequences of individual pairwise interactions inside a molecule. By creating a set of molecular fragments, we propose a composite energy method to explore changes in a molecule caused by removing selected nonbonded interactions between different molecular portions. Energies and forces are easily obtained with this composite approach, allowing geometry optimizations that lead to chemically meaningful structures that describe how the omitted interactions contribute to changes in the local geometrical minima. We illustrate the application of our new hybrid scheme by computing the influence of intramolecular hydrogen-bonding interactions in two small molecules: 1,6-($tG^+G^+TG^+G^+g^-$)-hexanediol and a cyclic analogue, *cis*-1,4-cyclohexanediol. The resulting structural and energetic changes are interpreted to yield key physical insights and quantify concepts such as “preparation energy” or “reorganization energy”. We demonstrate that the composite method can be extended to larger molecular systems by showing its application on a Si(100) surface model containing interactions between dissociated ammonia molecules on adjacent surface dimers. The scheme’s efficacy is also tested by applying it to systems having multiple intramolecular interactions, *viz.*, 3_{10} -polyglycine and H^+GPGG . Furthermore, the cooperative nature of intramolecular hydrogen bonds is explored by using interaction–deletion in 2-nitrobenzene-1,3-diol.



1. INTRODUCTION

A large portion of useful chemical and biochemical transformations have their origins not only in covalent bonding networks but also in weak interactions such as hydrogen bonding, electrostatic interactions, and dispersion interactions. From a range of applications such as protein folding,^{1,2} ionic solvation,^{3–5} and anion/cation binding,^{6–8} it is well recognized that a significant component of structural stability comes from such nonbonding interactions, typically involving energies <15 kcal mol^{−1}. Dipole–dipole, dipole–induced dipole, and other weak intermolecular forces often dictate chemical reactivity as well. Therefore, such noncovalent interactions are of significant interest to the chemistry community at large. Theoretical tools that can investigate and quantify the behavior of nonbonded interactions can lead to breakthroughs in understanding, design, and prediction of novel and important chemistry.

Noncovalent interactions can be broadly classified as either *intermolecular* or *intramolecular*. To fully understand the nature of these interactions across different molecular species, it is critical to develop schemes to quantify them by using appropriately designed theoretical models. Because interaction energies are relative energies, they are typically defined with

respect to a zero of energy (or a reference point); that is, the energy of a geometry where the concerned interaction is absent (or energetically zero). While computing an *intermolecular interaction* between two chemical species, the involved monomers at an infinite distance can be considered as a well-defined geometry at which the concerned interaction is nonexistent. Thus, the undisputed way to compute the energy associated with an *intermolecular interaction* is the so-called *supermolecular approach*,^{9,10} where the (intermolecular) interaction energy between two distinct species is defined as the difference between the energy of the complex formed from the two species and the sum of the energies of the two individual species. In contrast, *intramolecular interactions* occur between atom groups connected through a common molecular

Received: March 31, 2021

Revised: May 7, 2021

Published: May 20, 2021



backbone, making it impossible to form isolated monomer (donor/acceptor) entities, which in turn makes it difficult to construct a well-defined and unique reference geometry with respect to which intramolecular interaction energy could be computed. Consequently, numerous methods have been developed to quantify intramolecular interactions,¹¹ each proposing its own zero of energy, which in most cases depends on the type of molecule under study. Moreover, the lack of experimental data for quantifying intramolecular interactions further makes it difficult to validate any of the proposed methods definitively.^{12,13} Some of the popular fragment and conformation-based methods to compute intramolecular interactions are the open–close method,¹⁴ ortho–para method,¹⁵ cis–trans method,¹³ isodesmic/homodesmic reaction method,^{15,16} rotation barriers method (RBM),¹⁷ related rotamers method (RRM),^{18,19} molecular tailoring approach (MTA),^{20–25} and so on.²⁶ While many of these methods are quite effective, their applicability is typically restricted for a narrow class of problems. Wave-function-based methods like intramolecular SAPT (ISAPT)^{27–30} and natural bond orbital (NBO)³¹ compute the interaction energy directly. As with other methods, ISAPT requires a well-defined zeroth-order wave function representing the noninteracting monomers (equivalent to the zero of energy in conformation/fragment-based methods). Such a wave function has been defined in a couple of different ways without resorting to a cut-and-cap approach.^{28–30} Nevertheless, designating an appropriate linker region (which connects the acceptor and donor regions) is nontrivial as it needs to be defined in such a way so as not to have any noncovalent interactions with the donor and acceptor groups.³⁰ The NBO formalism defines the energy of a noncovalent interaction primarily in terms of the charge-transfer energy between donor and acceptor orbitals and hence does not incorporate contributions due to perturbations in the electron density from the molecular regions which are not in the immediate vicinity of the donor and acceptor groups.^{32,33} Qualitative (and visualization) methods, viz., noncovalent interactions (NCI),^{34,35} atoms-in-molecules (AIM),^{36,37} and electron localization function (ELF),^{38,39} make use of molecular electron density to estimate the strength and location of noncovalent interactions, thus providing a complementary way to study them.

The composite method described in this work is designed to identify specific nonbonded atom–atom interactions and effectively omit them in a manner reminiscent of some previous models, such as the isodesmic approach and the MTA. Although existing methods estimate the intramolecular bond strengths reasonably well, none of them directly predict the molecule's geometrical response in the absence of the concerned interaction. Our approach is to use composite energy models to *optimize geometrical parameters without selected noncovalent interactions*. We suggest a general composite method to essentially remove atom–atom interactions such as intramolecular hydrogen bonds from an *ab initio* or DFT-based calculations with the scheme defined below. Geometry optimizations using such a composite energy scheme are illustrative in understanding the nature of such weak interactions and their structural consequences. In addition, it provides a quantitative assessment of widely used concepts such as “preparation energy” or “reorganization energy”. The present work also attempts to untangle the cooperativity between intramolecular hydrogen bonds, which has mostly been studied previously only in the context of

intermolecular interactions.^{40,41} The presence of multiple intramolecular interactions in a molecule may have a strengthening or weakening effect on each other, which can lead to deviations in the hydrogen bond strengths from the normal trend.

2. METHOD

Hydrogen bonding represents a quintessential *intramolecular noncovalent interaction*—typically formed between the so-called donor and acceptor subunits of the same molecule. For example, in the hydrogen-bonded conformation of 1,6-hexanediol (Figure 1a), the two hydroxyl groups constitute

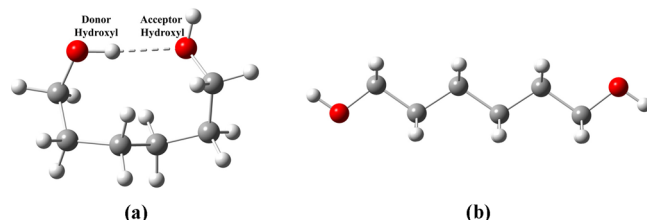


Figure 1. (a) 1,6-(tG⁺G⁺TG⁺G⁺g⁻)-hexanediol and (b) 1,6-(tTTTt)-hexanediol.

such a donor–acceptor pair. To effectively remove such a hydrogen-bonding interaction between a specified pair of atoms (or atom groups), the energies and forces of the molecular system of choice must be appropriately redefined. To achieve this, we define the *composite energy* of a molecule, obtained by leaving out the energy associated with the concerned intramolecular interaction, as

$$E(\text{composite}) = E(\text{full}) - E(\text{interaction}) \quad (1)$$

In the case of *intermolecular* hydrogen bonding, the interaction energy is uniquely defined as

$$E(\text{interaction}) = E(D \cup A) - E(D) - E(A) \quad (2)$$

Here, $E(D)$ and $E(A)$ represent the energies of donor and acceptor molecules, respectively, and $E(D \cup A)$ represents the energy of the hydrogen-bonded interaction complex. However, in the case of *intramolecular* hydrogen bonding, the donor and acceptor are not separate molecules and hence are not uniquely defined. Rather, the donor and acceptor represent subunits in the same molecule, and there can be potential *overlap* between them depending on the amount of backbone included in their representations. In such a case, the generalized interaction energy can be redefined as

$$E(\text{interaction}) = E(D \cup A) - E(D) - E(A) + E(D \cap A) \quad (3)$$

Here, $E(D)$ and $E(A)$ represent the energies of donor and acceptor *subsystems* (*vide infra*), respectively. In this description, the molecule containing an intramolecular hydrogen-bonding interaction is partitioned into donor, acceptor, and backbone (nonoverlapping) *fragments*, which are then combined to construct the requisite subsystems. In principle, different models can be constructed by including only parts of the backbone in the donor and acceptor subsystems. Although a rough estimate of the interaction energy can be obtained by using such smaller subsystem definitions, it may not be sufficient to represent the interaction energy accurately. In particular, the selected interactions contained in the full molecular system and the truncated subsystems may be

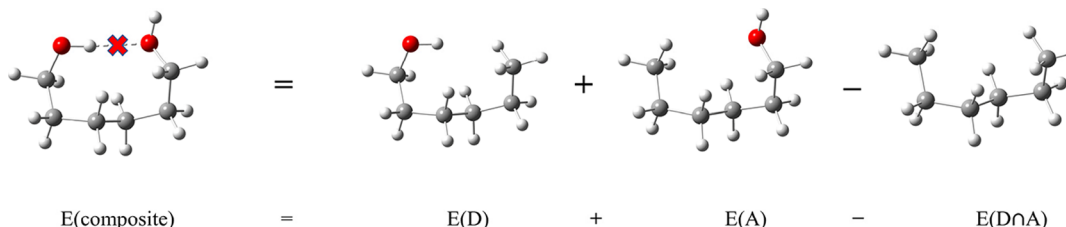


Figure 2. Pictorial representation of the proposed composite energy scheme for 1,6-(tG⁺G⁺TG⁺G⁺g⁻)-hexanediol.

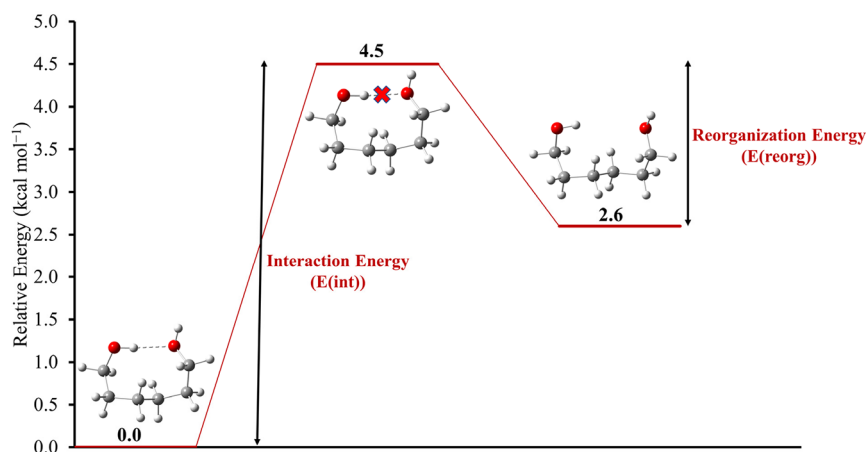


Figure 3. Energy profile of 1,6-(tG⁺G⁺TG⁺G⁺g⁻)-hexanediol obtained from comparisons between the standard MP2/aug-cc-pVDZ energy and geometry with those obtained from the composite energy scheme.

unbalanced due to having different chemical environments. This imbalance can be corrected by including the entire backbone in each subsystem (donor and acceptor), leading to a *well-defined composite method*. However, this leads to double counting of the overlapping part between the donor and acceptor subsystems (backbone). Specifically, the subsystem represented by $E(D \cap A)$ in eq 3 is nothing but a correction for double counting the backbone fragment of the molecule, common to both donor and acceptor subsystems. Moreover, $E(D \cup A)$ in such a case is $E(\text{full})$, the full energy of the interaction complex. Thus

$$E(\text{interaction}) = E(\text{full}) - E(\text{D}) - E(\text{A}) + E(\text{D} \cap \text{A}) \quad (4)$$

Substituting eq 4 in eq 1 leads to a simple expression for the composite energy.

$$\begin{aligned} E(\text{composite}) &= E(\text{full}) - E(\text{interaction}) \\ &= E(\text{D}) + E(\text{A}) - E(\text{D} \cap \text{A}) \end{aligned} \quad (5)$$

The composite energy scheme defined in this work, eq 5, is reminiscent of other fragment-based methods (viz., isodesmic method¹⁵ and MTA²²), where double counting of overlapping fragments is considered. In addition, whenever covalent bonds are broken, the unsatisfied valences have to be taken into account and are terminated with hydrogen link atoms.⁴² The link atoms utilize scale factors to give an appropriate bonding description, as in the standard ONIOM method.^{42,43} The gradients are also a composite sum of the gradients for each subsystem. Note that the link atom gradients are projected onto the host and supporting atoms as in ONIOM.⁴² The availability of gradients through the composite energy scheme allows for the possibility of minimizing (or optimizing) the composite energy, providing a relaxed structure that the

molecule would have preferred had the concerned interaction not been present there. This creates a simple implementation for the existing electronic structure software to perform energy evaluations and geometry optimizations. Frequencies and other higher-order properties of the interaction-deleted structure can also be computed through a composite sum of its constituent subsystem's properties and are described in detail elsewhere.⁴⁴ Therefore, our novel method can explore the energetic and geometric consequences of noncovalent interactions between two atoms (or atom groups). The method is general and can be used with any *ab initio* or density functional approach.

2.1. Illustrative Example: 1,6-Hexanediol. The tG⁺G⁺TG⁺G⁺g⁻ conformation of 1,6-hexanediol⁴⁵ (Figure 1a), having only a single isolated intramolecular hydrogen bond, serves as an ideal system to illustrate the working of the *interaction-deletion* protocol outlined above. The hydrogen-bonding distance in the standard MP2/aug-cc-pVDZ^{46,48} optimized structure for tG⁺G⁺TG⁺G⁺g⁻ conformer is 2.04 Å. This is in the typical range of OH···O distances observed in water clusters, 1.8–2.0 Å, indicating a reasonably strong hydrogen bond. In fact, the presence of this hydrogen bond makes this conformation to be more stable than the all-trans conformation (Figure 1b) by 2.6 kcal mol⁻¹ at the MP2/aug-cc-pVDZ level of theory, reversing the order seen for the parent hexane where the trans conformation is more stable by 0.9 kcal mol⁻¹.

To obtain the hydrogen-bond energy and the structural response if the said interaction is deleted, a composite energy scheme for the concerned system is constructed (via eq 5), which is pictorially depicted in Figure 2. As shown in Figure 2, the donor subsystem (D) constitutes the donor hydroxyl and the full alkane backbone, while the acceptor subsystem (A) is composed of acceptor hydroxyl and the carbon backbone. To

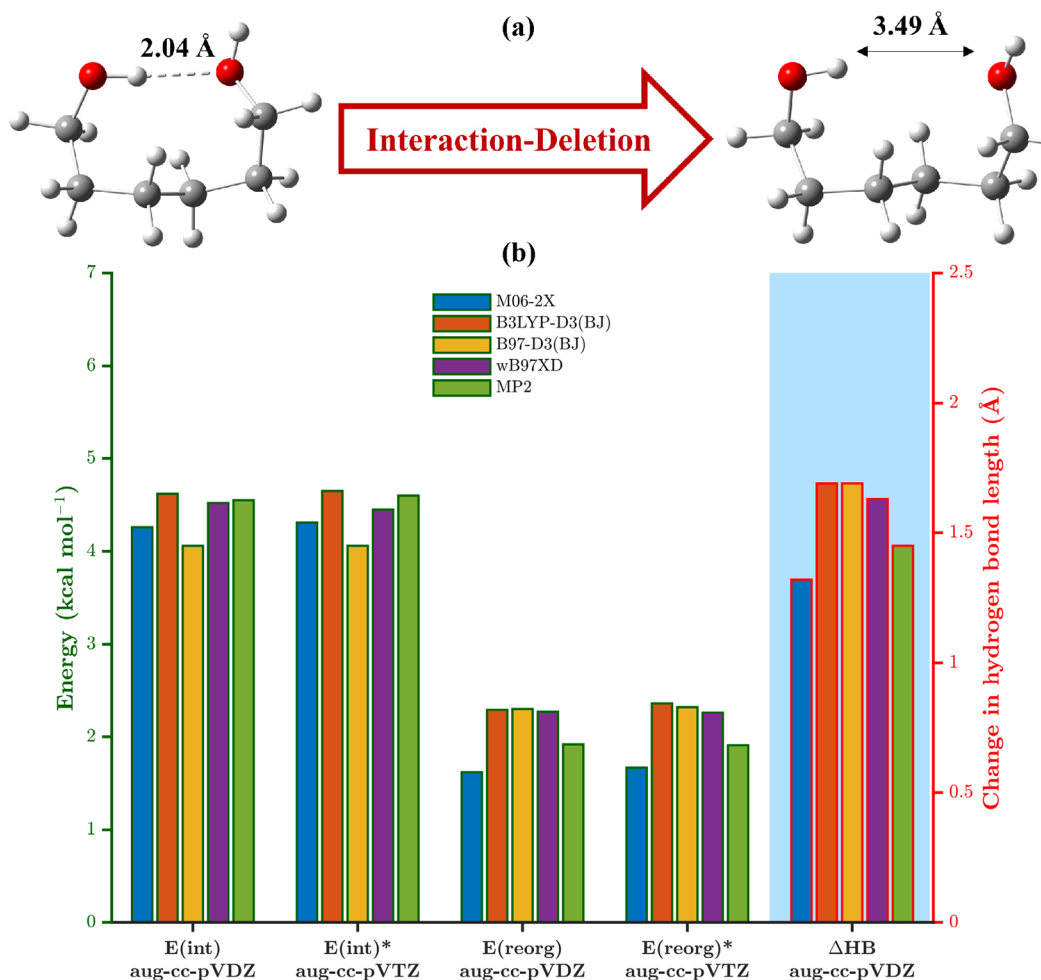


Figure 4. (a) Optimized geometry of 1,6-(tG+G+TG+G+g-)-hexanediol before (left) and after (right) interaction-deletion. (b) Bar graph depicting interaction energy ($E(\text{int})$), reorganization energy ($E(\text{reorg})$), and change in hydrogen bond length (ΔHB) at the indicated level of theory. Asterisks (*) indicate that only the single-point energies were calculated with aug-cc-pVTZ using the aug-cc-pVDZ optimized geometries.

keep the number of atoms consistent in the scheme, the energy of the alkyl backbone ($E(D \cap A)$) is subtracted from the sum of the energies of the donor and acceptor subsystems. It is apparent from the energy scheme (Figure 2) that the only major interaction being left out is the intramolecular hydrogen bond between the two terminal hydroxyls. Using eq 4, we evaluated the energy associated with the intramolecular hydrogen bond in 1,6-(tG⁺G⁺TG⁺G⁺g⁻)-hexanediol to be 4.55 kcal mol⁻¹ at the MP2/aug-cc-pVDZ level of theory (Figure 3). The relevant hydrogen bond energies with some of the popular DFT functionals (viz., M06-2X,⁴⁹ B3LYP-D3(BJ),⁵⁰⁻⁵³ B97-D3(BJ),^{50,51,54,55} and ω B97X-D⁵⁶) are also reported in Figure 4b in the form of a bar graph. Interestingly, the hydrogen bond energies obtained from B3LYP-D3(BJ) and ω B97X-D turned out to be quite close to that from MP2.

The fully optimized molecular geometry (at which the composite energy is computed) is not optimum for an *interaction-deleted* structure. Because the forces for each of the fragments are readily available, a composite energy optimization can be performed (starting from the fully optimized geometry) to obtain a relaxed structure that is more representative of a geometry without an intramolecular hydrogen bond (Figure 4a). The energy change associated with the geometrical deformation that the molecule undergoes during the composite energy optimization can be termed as the

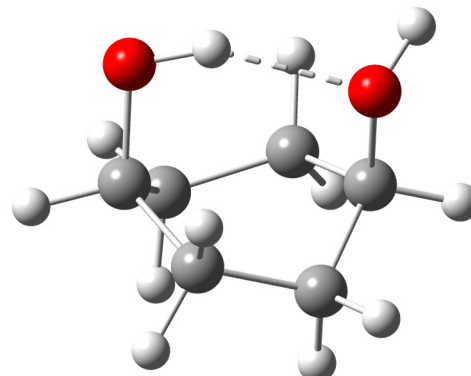


Figure 5. Twist-boat cis-1,4-cyclohexanediol.

preparation energy or *reorganization energy*. From another perspective, it is essential to note the significant strain in 1,6-hexanediol (Figure 1a) since it has to adopt a structure conducive to the formation of the hydrogen bond. Consequently, the molecular backbone has to distort sufficiently to allow the atoms involved in the hydrogen bond to point toward each other at a close enough distance to interact in a stabilizing manner. Thus, the energy associated with the change in molecular structure to attain an appropriate

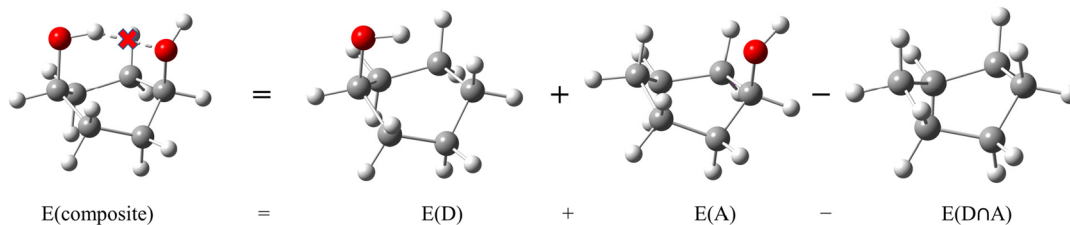


Figure 6. Pictorial representation of the composite energy scheme for *twist-boat cis-1,4-cyclohexanediol*.

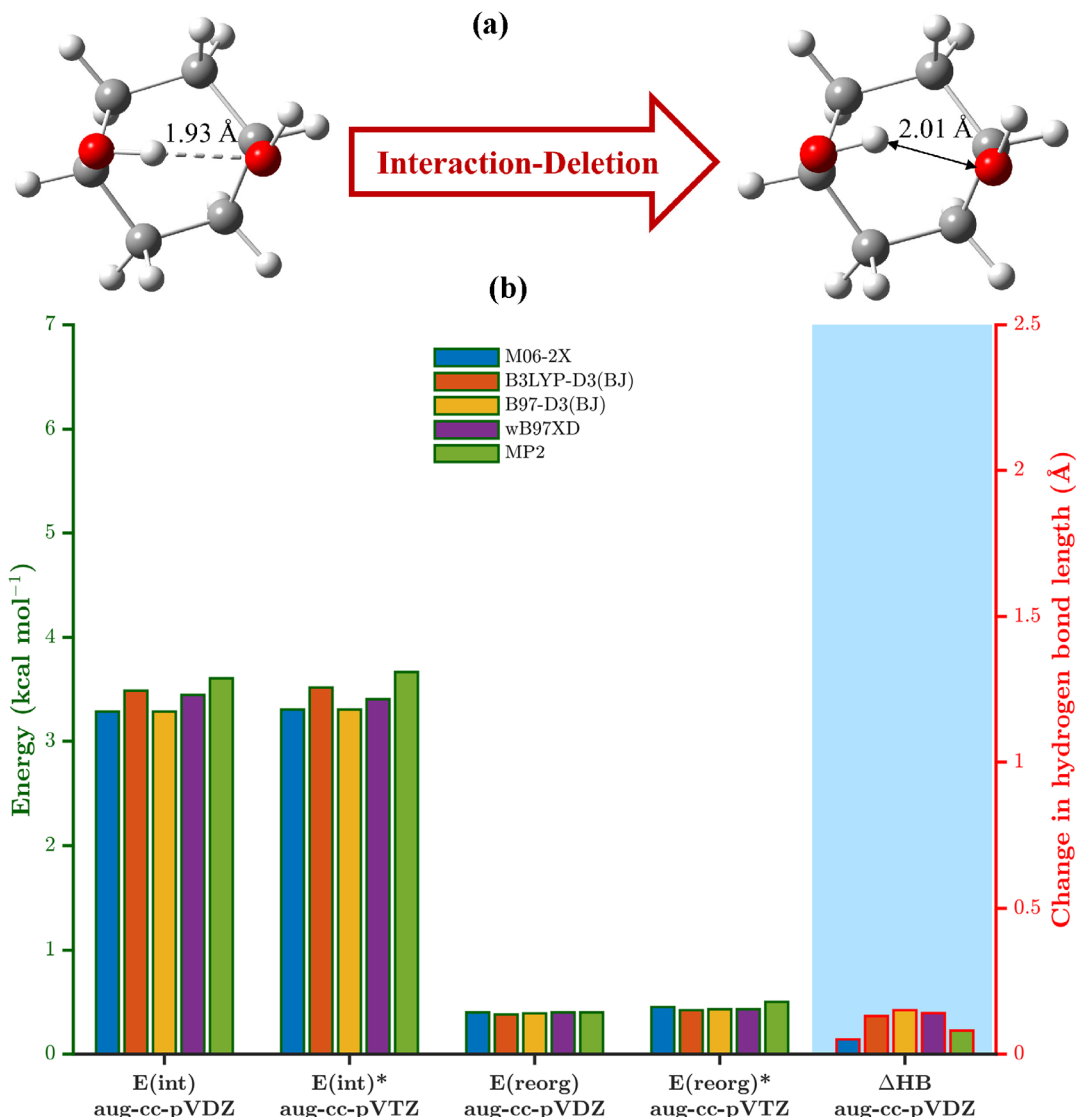


Figure 7. (a) Optimized geometry of *twist-boat cis-1,4-cyclohexanediol* before (left) and after (right) interaction-deletion (at MP2/aug-cc-pVDZ). (b) Bar graph depicting interaction energy ($E(\text{int})$), reorganization energy ($E(\text{reorg})$), and change in hydrogen bond length (ΔHB) at the indicated level of theory. Asterisks (*) indicate that only single-point energies were calculated with aug-cc-pVTZ using the aug-cc-pVDZ optimized geometries.

conformation that enables the feasibility of the intramolecular interaction is termed as the *reorganization energy* ($E(\text{reorg})$) (Figure 3). This can also be thought of as an energy penalty due to molecular strain that partially offsets the stabilization energy due to the hydrogen bond formation.

The geometrical parameter expected to change the most during the composite energy optimization is the hydrogen bond length itself since it is directly associated with the existence of a hydrogen bond in a molecule. As such, the

change in hydrogen bond length (ΔHB) is usually observed to be directly proportional to the reorganization (or preparation) energy. In the present case, the two hydroxyls moved apart by ~ 1.5 Å, thus contributing an energy penalty of ~ 2 kcal mol⁻¹ (Figure 4b). The lack of interaction between the two hydroxyl groups can be analyzed in terms of some other key geometrical parameters as well. The most useful geometrical parameter that illustrates the nature of the backbone distortion is $C_1 \cdots C_6$ distance which increases by ~ 0.6 Å, indicating an overall

relaxation in the molecular geometry. Additionally, the O–H bond distance of the donor hydroxyl group decreases from 0.974 to 0.967 Å, consistent with the lack of a hydrogen bond. Finally, the optimized geometries obtained at the double- ζ basis (aug-cc-pVDZ) are also subjected to corresponding single-point energy evaluations at the triple- ζ basis (aug-cc-pVTZ^{47,48}) to obtain improved relative energies. However, the interaction and preparation energies were found to vary negligibly between the double- and triple- ζ basis sets (Figure 4b).

The elimination of the intramolecular hydrogen bond affects its infrared fingerprint as well. In the present example of 1,6-hexanediol, the stretching frequency associated with the donor hydroxyl is at 3683.0 cm⁻¹ (computed at MP2/aug-cc-pVDZ), quite different from that for the acceptor hydroxyl (3813.2 cm⁻¹). This is consistent with the red-shifted frequency pattern usually observed for a hydrogen-bonded (donor) group and is widely recognized as the signature of a hydrogen-bonding interaction.^{57,58} However, upon performing a normal-mode analysis on the *reorganized* interaction-deleted structure, we found both hydroxyls to vibrate with similar frequencies (3816.3 and 3827.6 cm⁻¹), indicating the absence of any interaction between the two groups.

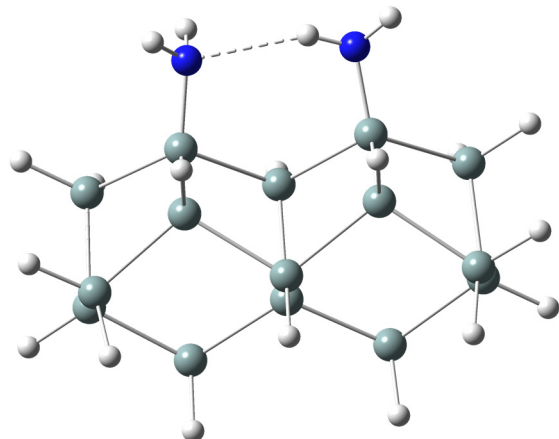


Figure 8. Two ammonia adsorbates dissociated on a Si₁₅H₁₆ cluster.

3. COMPUTATIONAL DETAILS

All calculations were performed by using the Gaussian 16⁵⁹ set of programs. For each system being investigated, the geometries were initially optimized to minimize the traditional electronic energy corresponding to the chosen level of theory. These structures were then used for single-point evaluations

with our new composite energy scheme to evaluate the strength of the intramolecular interaction at this geometry. Finally, and most importantly, geometry optimizations were performed in all systems to minimize the composite energy discussed above. This provides the preferred geometry for the system where the chosen interaction is “turned off” while keeping the rest of the molecular interactions intact. For smaller systems (viz., *twist-boat* 1,4-cyclohexanediol), computations are done at both MP2 and DFT levels of theory, while for larger systems (viz., Si₁₅H₁₆·2NH₃ and 3₁₀-polyglycine), only density functional theory is used to evaluate interaction and reorganization energies.

4. RESULTS AND DISCUSSION

4.1. *Twist-Boat cis-1,4-Cyclohexanediol.* The *twist-boat* conformation of *cis*-1,4-cyclohexanediol (Figure 5) allows an intramolecular hydrogen bond across the ring system.^{60,61} When this molecule is in the *twist-boat* conformation, hydrogen bonding occurs when the hydroxyl groups are appropriately pointed toward each other. A corresponding composite energy scheme is constructed to understand the energetic and geometric consequences of removing this hydrogen bond, as shown in Figure 6. The composite energy model (through the use of eq 5) estimates the strength of the concerned hydrogen bond to be around 3.5 kcal mol⁻¹ across all levels of theory used (Figure 7b). Interestingly, at the fully optimized geometry (at MP2/aug-cc-pVDZ), the hydrogen bond length is 1.93 Å, even shorter than that in 1,6-hexanediol (2.04 Å). Therefore, despite *cis*-1,4-cyclohexanediol having a shorter hydrogen bond, its strength is somewhat weaker than that in 1,6-hexanediol, which contrasts with the commonly observed correlation between bond lengths and bond strengths.^{62,63} This implies that the proximity of the two hydroxyl groups is not merely associated with the hydrogen bond strength but is also a conformational necessity. We then considered the geometric consequences of removing the intramolecular hydrogen bond in *cis*-1,4-cyclohexanediol. Most notably, the OH···O distance increases slightly from 1.93 to 2.01 Å, a change of only 0.08 Å (Figure 7a), which is also the largest deviation in any of the geometrical parameters for the concerned molecule. Hence, not surprisingly, the reorganization energy turns out to be relatively low (~0.5 kcal mol⁻¹), further indicating that the molecule prefers a similar geometry even in the absence of the intramolecular hydrogen bond.

Traditional MP2/aug-cc-pVDZ optimizations of the *chair* and *twist-boat* conformations of cyclohexane predict a 6.2 kcal mol⁻¹ preference for the *chair* conformer, in agreement with a previously reported MP2 relative energy.⁶⁴ In the presence of

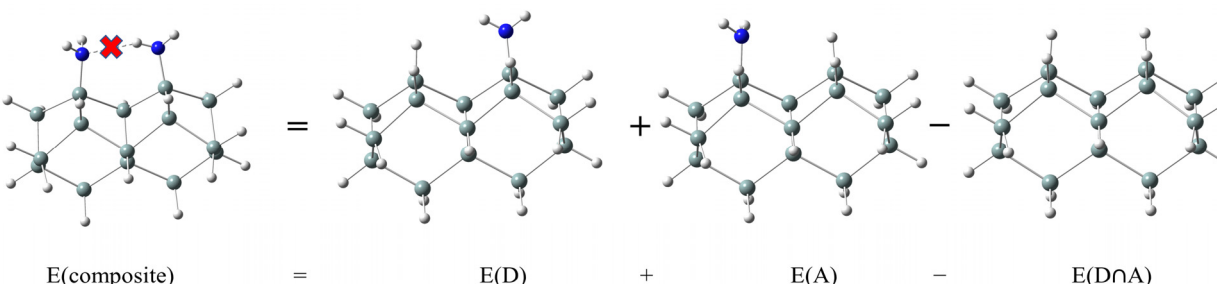


Figure 9. Pictorial representation of the proposed composite energy scheme for two ammonia dissociated on Si(100).

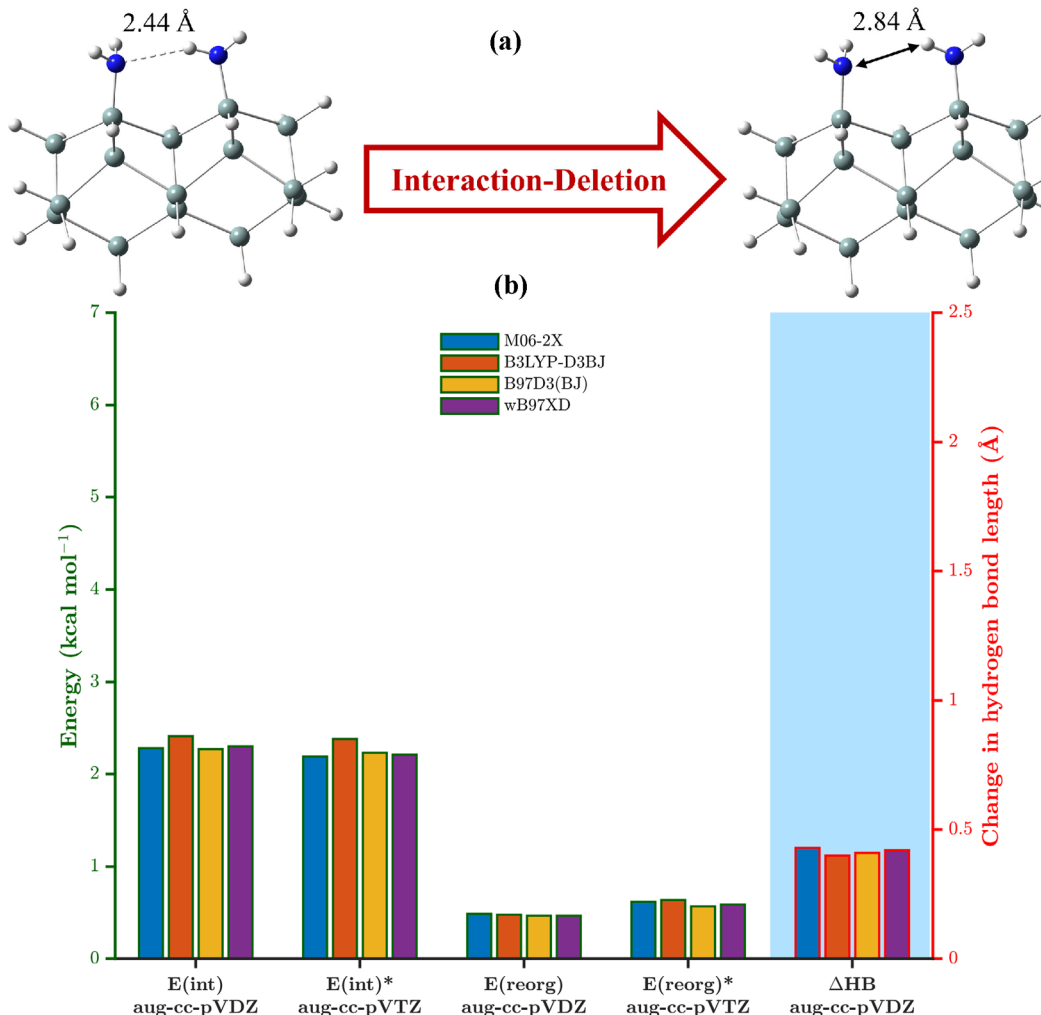


Figure 10. (a) Optimized geometry of $\text{Si}_{15}\text{H}_{16} \cdot 2\text{NH}_2$ before (left) and after (right) interaction-deletion (at B3LYP-D3(BJ)/aug-cc-pVDZ). (b) Bar graph depicting interaction energy ($E(\text{int})$), reorganization energy ($E(\text{reorg})$), and change in hydrogen bond length (ΔHB) at the indicated level of theory. Asterisks (*) indicate that only the single-point energies were calculated with aug-cc-pVTZ using the aug-cc-pVDZ optimized geometries.

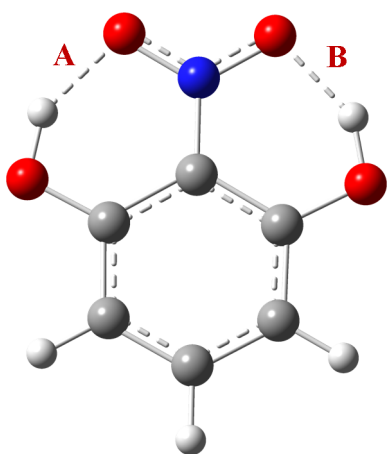


Figure 11. 2-Nitrobenzene-1,3-diol. The two intramolecular hydrogen bonds are labeled as A and B.

hydrogen bonding, the preference for the chair structure decreases to $3.9 \text{ kcal mol}^{-1}$. Our analysis suggests that part of this decrease is due to hydrogen bonding while the rest are probably due to the intrinsic effects of substitution. The

vibrational frequency associated with the donor hydroxyl shifted from 3670.3 to 3812.2 cm^{-1} upon interaction-deletion, characteristic of the difference between the frequencies for hydrogen-bonded and non-hydrogen-bonded species.

4.2. Ammonia Adsorption on Si(100). The composite energy method can be used to study larger systems as well. To demonstrate its capability as a tool to elucidate weak interactions on surface models, we modeled the dissociation products of ammonia molecules on a fully relaxed $\text{Si}_{15}\text{H}_{16}$ cluster model representing two adjacent dimers on the Si(100) surface (Figure 8).^{65,66} Coverage dependence has been experimentally shown to be associated with shifts of the Si-H stretching frequencies of the dissociated ammonia.^{67–71} This molecular system is used as an example to show how our composite energy method can be used to quantify and describe the energetic changes and geometric distortions that occur as nearby adsorbates interact at higher coverages.

When two ammonia adsorbates dissociate on a Si(100) dimer row, one hydrogen bond is formed, whose strength is estimated to be around $2.3 \text{ kcal mol}^{-1}$ (Figure 10b) by using the composite energy scheme shown in Figure 9, indicating a relatively weak hydrogen bond, in line with the typical hydrogen bond strength among amino groups. Performing a

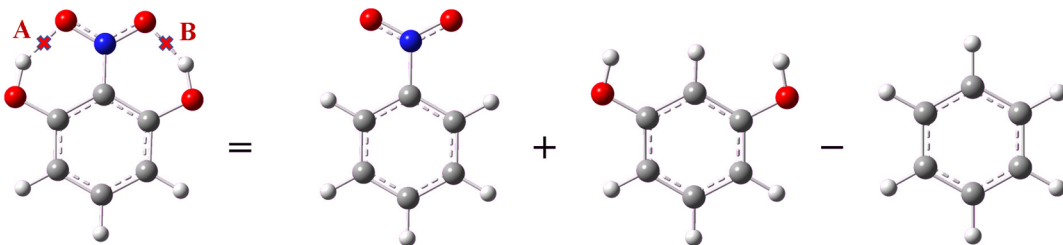


Figure 12. Composite energy scheme for the simultaneous deletion of hydrogen bonds A and B in 2-nitrobenzene-1,3-diol.

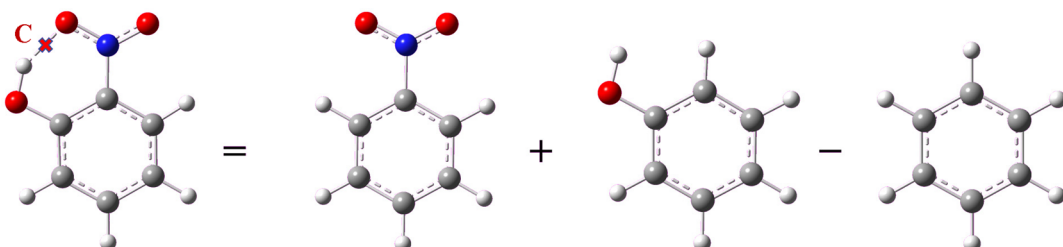


Figure 13. Composite energy scheme for the deletion of the intramolecular hydrogen bond in *o*-nitrophenol.

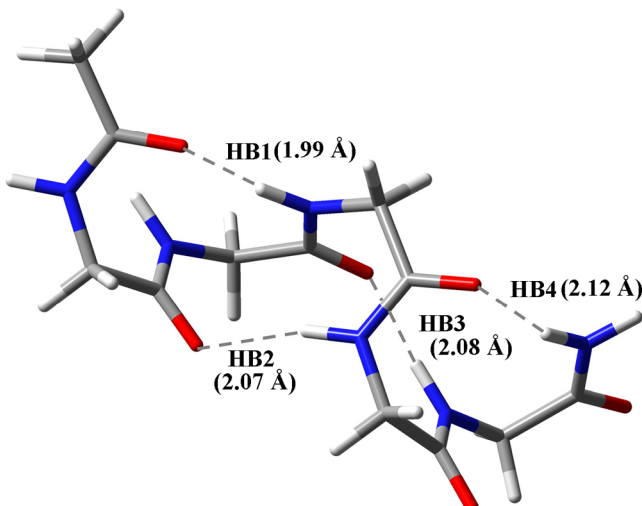


Figure 14. Structure of 3₁₀-polyglycine (GGGGG). Intramolecular hydrogen bond lengths are shown at the ω B97X-D/aug-cc-pVQZ level of theory.

geometry optimization using our composite energy method shows the relaxation of the geometry without the interdimer hydrogen bond. At the B3LYP-D3(BJ)/aug-cc-pVQZ level of theory, the hydrogen bond length is 2.44 Å, which increased to

2.84 Å after composite energy optimization (Figure 10a). The strain energy in the adsorbate is now decreased in the absence of any stability from the formation of a hydrogen bond. A second notable geometric parameter is the donor N–H bond distance, with values of 1.015 and 1.019 Å for the composite optimized and fully optimized systems, respectively. The slight decrease in the bond length with the composite approach is consistent with simple expectations since the weak hydrogen bond interaction has been effectively omitted. Because the silicon cluster did not have to undergo a large geometric distortion for the hydrogen bond to stabilize the system's total energy, the associated reorganization energy is quite small (of the order of 0.5 kcal mol⁻¹, shown in Figure 10b).

4.3. Hydrogen Bond Cooperativity: Conjoined Intramolecular Hydrogen Bonds. It is worth looking at a few more interesting cases of intramolecular interactions; for instance, when a lone donor (or acceptor) unit is associated with multiple hydrogen bonds, potentially giving rise to cooperative effects between the involved interactions.^{40,41} A simple example of such a system is 2-nitrobenzene-1,3-diol (Figure 11), where the nitro group is acting as the sole acceptor of the hydrogen bonds from the two neighboring hydroxyls. Let us designate the two intramolecular hydrogen bonds as A and B, as shown in Figure 11. The interaction–deletion scheme (shown in Figure 12) involving a simultaneous deletion of both interactions (A + B) assigns a value of

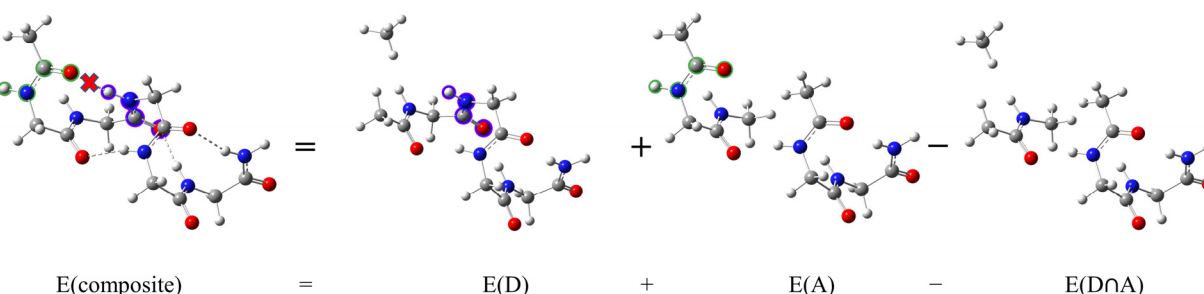


Figure 15. Pictorial representation of the proposed composite energy scheme for 3₁₀-polyglycine. The peptide groups represent the donor/acceptor fragments.

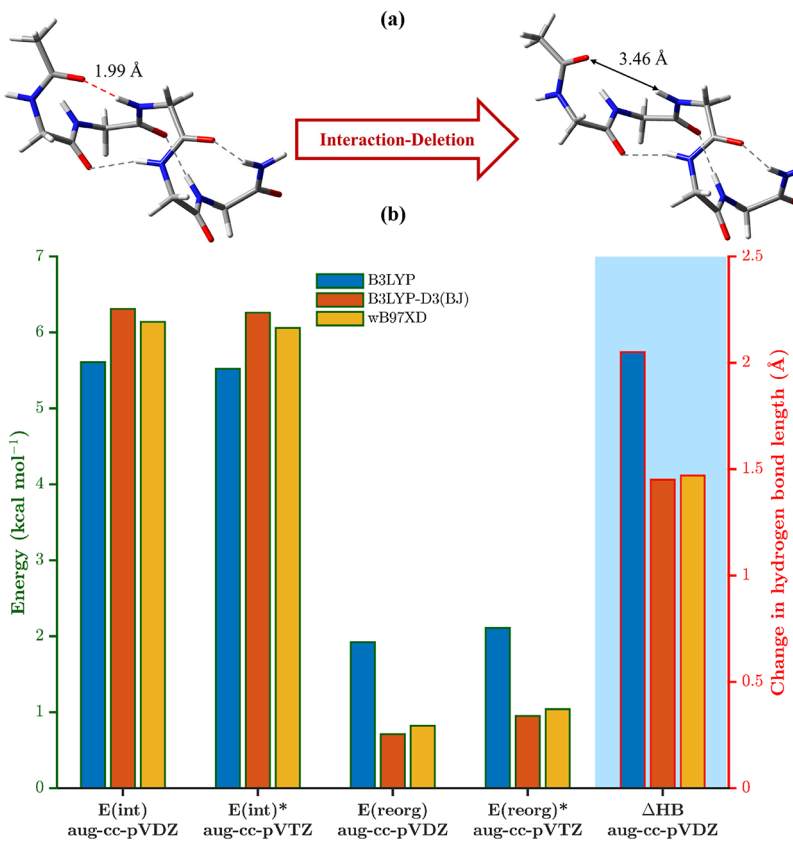


Figure 16. (a) Optimized geometry of GGGGG before (left) and after (right) deletion of HB1 (at ω B97X-D/aug-cc-pVDZ). (b) Bar graph depicting interaction energy ($E(\text{int})$), reorganization energy ($E(\text{reorg})$), and change in hydrogen bond length (ΔHB) at the indicated level of theory. Asterisks (*) indicate that only the single-point energies were calculated with aug-cc-pVTZ using the aug-cc-pVDZ optimized geometries.

16.25 kcal mol⁻¹ (at B97D3/aug-cc-pVDZ) to the sum of the two hydrogen bonds. All the subsequent energy values provided in this section were obtained at B97D3/aug-cc-pVDZ level of theory.

To determine the nature of cooperativity in play, it is imperative to compare the interaction energy of the conjoined hydrogen bonds with their isolated counterparts. Because the nitro group participates in both hydrogen bonds, we have adopted a slightly modified procedure to get the strengths of the individual bonds. We have removed one of the hydroxyl groups to determine the intrinsic strength of a single intramolecular hydrogen bond in *o*-nitrophenol (Figure 13). In this case, the interaction energy of the intramolecular hydrogen bond (C) in *o*-nitrophenol (at the optimized geometry of 2-nitrobenzene-1,3-diol) is determined to be 8.71 kcal mol⁻¹. Therefore, the interaction energy associated with two such interactions (C) would be $8.71 + 8.71 = 17.42$ kcal mol⁻¹, which is more than the combined interaction energy of such an interaction present simultaneously in a molecule, i.e., 16.25 kcal mol⁻¹ (A + B). This suggests negative cooperativity and is in line with the physical/chemical nature of such interactions. Indeed, having the nitro group as the sole acceptor for two intramolecular hydrogen bonds would dilute electron density on both the acceptor oxygen atoms (of the nitro group), leading to the oxygen atoms being less polarized. This in turn makes the hydrogen bonds weaker compared to the case when only one such interaction is present, where the acceptor oxygen involved in the hydrogen bonding can accumulate relatively more negative charge (or electron

density), resulting in a more polarized and hence stronger hydrogen bond.

4.4. Nonterminal Hydrogen Bonds: 3₁₀-Polyglycine (GGGGG). Many molecules of practical interest have multiple intramolecular interactions holding the molecular conformation together, ultimately governing their structure and function. Therefore, it is of utmost importance to decipher how a specific intramolecular interaction contributes to the stability and conformation of a given molecule in response to the switching-off of that interaction, which in turn may provide insight into the folding–unfolding mechanism in protein-like molecules. Thus, it is of interest to assess the performance of the proposed composite energy model on a complex molecule having multiple intramolecular interactions.

An additional important factor to consider is that, thus far, we have considered only terminal units such as hydroxyl groups participating in hydrogen bonds, and it is relatively straightforward to set up schemes to “remove” them and consider the resulting energetic and structural implications. This is mainly due to the fact that such terminal groups are connected to the rest of the molecule by a single bond and can be replaced by a hydrogen “link atom”, as is typical when dealing with such bond truncations. However, in many cases, including peptides, the groups participating in hydrogen bonds, such as O=C or H–N, are attached to the rest of the molecule by two bonds and need two hydrogen link atoms to take care of the bond truncations. Because both hydrogens represent the same heavy atom being removed, the hydrogens would be unphysically close, potentially leading to artifacts. Deshmukh and Gadre²⁵ have developed an effective solution

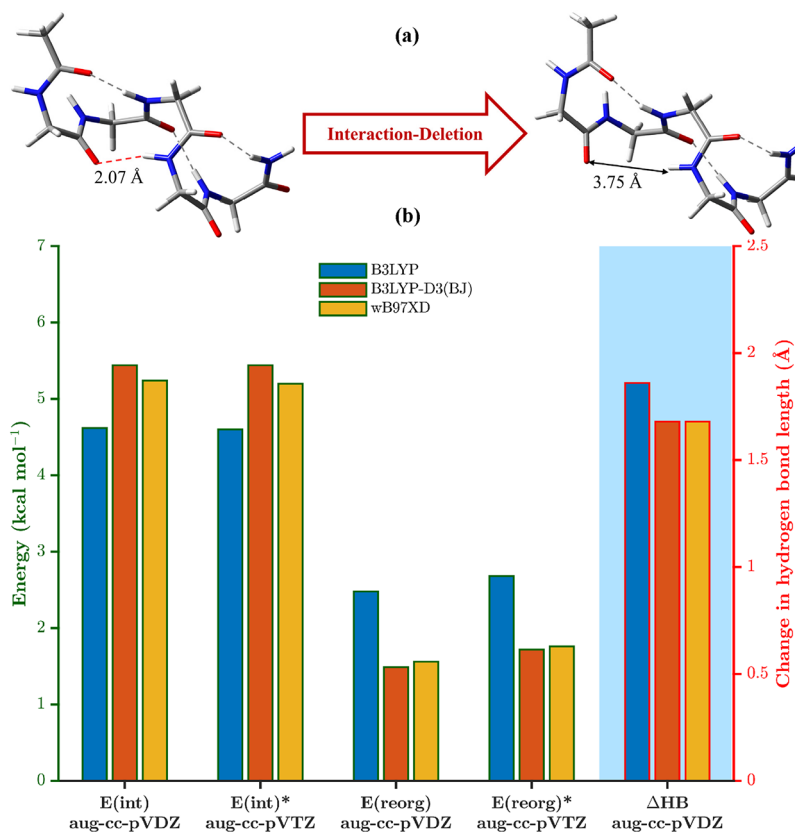


Figure 17. (a) Optimized geometry of GGGGG before (left) and after (right) deletion of HB2 (at ω B97X-D/aug-cc-pVDZ). (b) Bar graph depicting interaction energy ($E(\text{int})$), reorganization energy ($E(\text{reorg})$), and change in hydrogen bond length (ΔHB) at the indicated level of theory. Asterisks (*) indicate that only the single-point energies were calculated with aug-cc-pVTZ using the aug-cc-pVDZ optimized geometries.

to handle such issues by considering larger structural units for removal, and we have followed their approach to define the acceptor and donor fragments.

To illustrate these aspects, 3_{10} -pentaglycine (GGGGG) with a terminal acetyl group (instead of the carboxyl group) was chosen as the test system (Figure 14). GGGGG has four intramolecular hydrogen-bonding interactions responsible for its helical conformation. Henceforth, those four intramolecular hydrogen bonds are referenced as HB1 (shorthand for hydrogen bond-1), HB2, HB3, and HB4, as shown in Figure 14. In contrast to the previous test cases, the intramolecular interactions in the current system occur between atom groups that are part of the molecular backbone itself and not with atoms only at terminal positions. Consequently, the identity of the donor, acceptor, and backbone fragments may not be unique but can be made flexible as needed for benchmarking purposes. However, an appropriate composite energy scheme for nonterminal hydrogen bonds should satisfy the following two criteria. First, the size of the donor/acceptor subsystem must be large enough (or equivalently, the size of the donor/acceptor *fragment* must be small enough) to retain as much of the chemical environment of the parent molecule as possible in the scheme definition. Second, the distance between the hydrogen link atoms in the resulting donor and acceptor subsystems should not be unrealistically close, which may otherwise create artifacts while computing energies and gradients. The smallest donor/acceptor fragments that satisfy these two conditions are the peptide groups (CO–NH) participating in the hydrogen bond formation, and hence they can be used to formulate a composite energy scheme. We note

that such a scheme has already been proposed previously by Deshmukh and Gadre.²⁵ For the sake of brevity, the composite energy scheme is shown for HB1 only (Figure 15); however, the schemes corresponding to the remaining hydrogen bonds can be obtained following the same ideas and are depicted in the Supporting Information (Figures S1–S3).

Each of the four hydrogen bonds is deleted one at a time, and the respective energetic and geometric consequences are studied and summarized in the form of bar charts (Figures 16b, 17b, 18b, and 19b). Among the DFT functionals chosen to examine this system, there is a clear contrast between the results obtained with dispersion-corrected functionals (viz., B3LYP-D3(BJ) and ω B97X-D) and the functional without any dispersion term (viz., B3LYP). The interaction energy values obtained with B3LYP (4.5–5.6 kcal mol⁻¹) are in agreement with the previously reported values by Deshmukh et al.²⁵ at B3LYP/6-311++G(d,p) using the MTA approach. The interaction energies obtained with B3LYP are around 0.5–1.5 kcal mol⁻¹ lower than those obtained with other functionals. The slightly lower values of interaction energies (with B3LYP) stems from the lack of any explicit dispersion term in B3LYP, which is known to be crucial for the correct description of noncovalent interactions. Therefore, in the B3LYP picture, noncovalent interactions are not as strongly bound as in the dispersion-corrected scenario, thus slightly underestimating the interaction energies. Extrapolating the trend seen for 1,6-hexanediol and *cis*-1,4-cyclohexanediol, the interaction energies obtained with B3LYP-D3(BJ) and ω B97X-D are expected to be much closer to those computed with MP2.

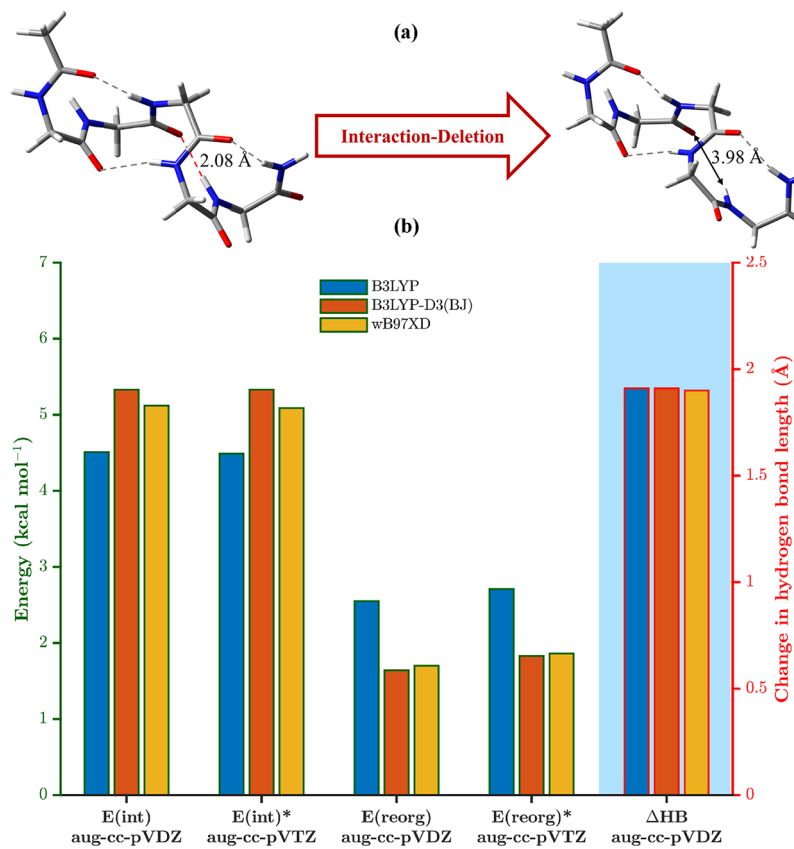


Figure 18. (a) Optimized geometry of GGGGG before (left) and after (right) deletion of HB3 (at ω B97X-D/aug-cc-pVDZ). (b) Bar graph depicting interaction energy ($E(\text{int})$), reorganization energy ($E(\text{reorg})$), and change in hydrogen bond length (ΔHB) at the indicated level of theory. Asterisks (*) indicate that only the single-point energies were calculated with aug-cc-pVTZ using the aug-cc-pVDZ optimized geometries.

The length of HB1 is slightly shorter than the rest of the hydrogen bonds, and hence it is also a bit stronger energetically, potentially due to having better directionality between donor–acceptor groups. Specifically, HB1 measures at around 2.0 Å and is worth over 6 kcal mol⁻¹ across all levels of theory used, while the rest of the three hydrogen bonds fall in the range 2.05–2.10 Å and are energetically worth around 5.5 kcal mol⁻¹. As expected, deletion of a hydrogen bond is accompanied by an increase in distance between the involved donor and acceptor atom groups, which results in slight uncoiling of the helical conformation, thus resulting in a loss in helicity of the peptide molecule. In previous examples, the reorganization energy was seen to be proportional to the change in hydrogen bond length; however, the present case being a relatively complex structure with multiple interactions, the relaxation of other geometrical parameters also contributes to the reorganization energy, resulting in deviations from the simple trend.

4.5. Conjoined and Nonterminal Intramolecular Hydrogen Bonds: H⁺GPGG. Hydrogen bonds where a single donor/acceptor group is being shared with multiple acceptors/donors are ubiquitous in nature, especially in biomolecules. One such example is *cis*-c1 H⁺GPGG (the protonated form of a tetrapeptide consisting of glycine, proline, glycine, and glycine, Figure 20), where the terminal NH₃⁺ group acts as a hydrogen bond donor for two carbonyl acceptors.⁷² Simultaneous deletion of both of these interactions using an appropriate interaction–deletion scheme (shown in Figure S4) provides an accumulated interaction energy of 26.8 kcal mol⁻¹. The relatively high value of the interaction energy is

consistent with the fact that the species is a *protonated structure*, and hydrogen bonding is much stronger in the case of charged systems. Subsequent optimization of the molecule in the absence of these interactions yields an unexpectedly high “reorganization energy” of 22.5 kcal mol⁻¹. This value is too high to result simply from structural relaxation effects. However, a careful inspection of the resulting geometry provides a simple explanation. When the two interactions are removed, optimization yields a geometry where the terminal NH₃⁺ is now free to make hydrogen bonds with the two previously noninteracting carbonyl groups, as shown in Figure 21. The molecule stabilizes significantly due to the *new hydrogen bond formations*, thus yielding a seemingly high “reorganization energy” (22.5 kcal mol⁻¹). Thus, the “reorganization energy” in this case includes the amount of stability achieved by the interaction-deleted structure through the formation of new noncovalent interactions in addition to simple geometrical relaxation.

Interaction–deletion thus provides a means to explore stationary points that may otherwise be hidden due to being overwhelmed by the most dominant interactions. In the present example of *cis*-c1 H⁺GPGG, switching off the two strong hydrogen bonds forced the molecule to a different potential energy minimum (in the full configuration space) containing two new hydrogen bonds where one of them is an intramolecular hydrogen bond between the two molecular arms (Figures 21 and 22). Further subjecting the resultant molecular geometry to an interaction–deletion optimization (by deleting an intramolecular hydrogen bond as shown in Figure 22) provides a conformation with the two original

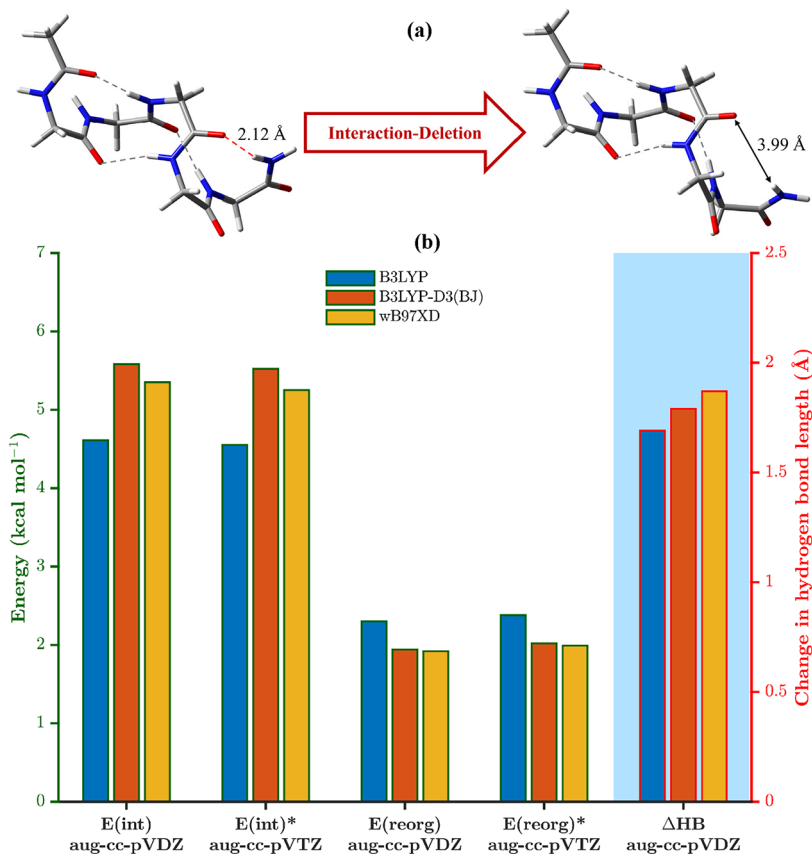


Figure 19. (a) Optimized geometry of GGGGG before (left) and after (right) deletion of HB4 (at ω B97X-D/aug-cc-pVDZ). (b) Bar graph depicting interaction energy ($E(\text{int})$), reorganization energy ($E(\text{reorg})$), and change in hydrogen bond length (ΔHB) at the indicated level of theory. Asterisks (*) indicate that only the single-point energies were calculated with aug-cc-pVTZ using the aug-cc-pVDZ optimized geometries.

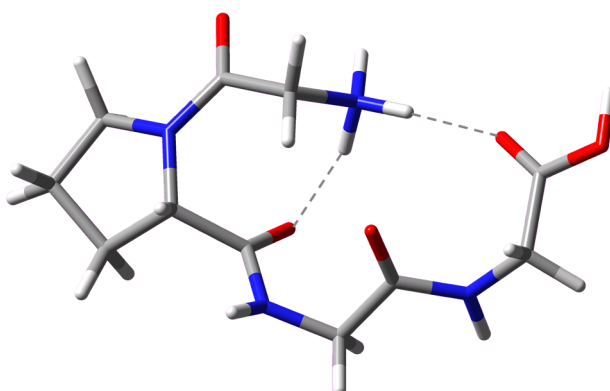


Figure 20. Molecular structure of *cis*-c1 H^+ GPGG. The structure has two intramolecular hydrogen-bonding interactions.

intramolecular hydrogen bonds reinstated, however, with the orientation of one of the peptide linkages flipped (Figure 22). This structure is a minimum only in the subspace defined by the fragments of its parent molecule; however, performing a full optimization brings it back to the original conformation of *cis*-c1 H^+ GPGG, thus completing the cycle. These techniques can be further expanded to explore the potential energy surface of complex molecules in a way complementary to traditional methods.

5. CONCLUSIONS

We have proposed a novel composite scheme that can be utilized to understand the energetics of weak interactions such as hydrogen bonds and their contributions to the associated strain energies in molecular systems. The specific atom–atom

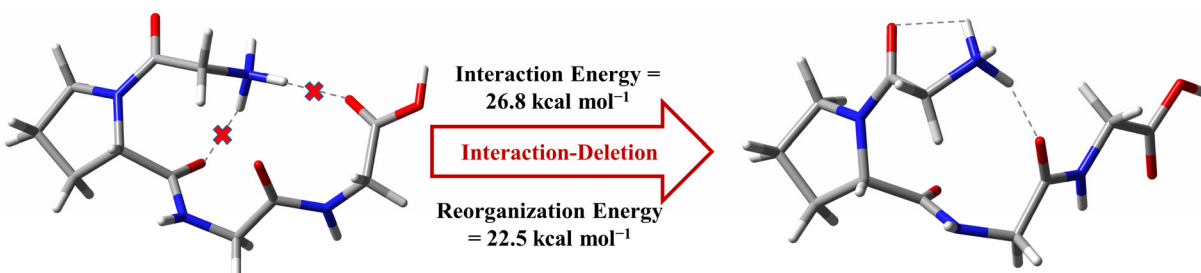


Figure 21. Optimized geometry of *cis*-c1 H^+ GPGG before (left) and after (right) deletion of the two depicted intramolecular hydrogen bonds (at B97D3/aug-cc-pVDZ). The corresponding composite energy scheme is shown in Figure S4.

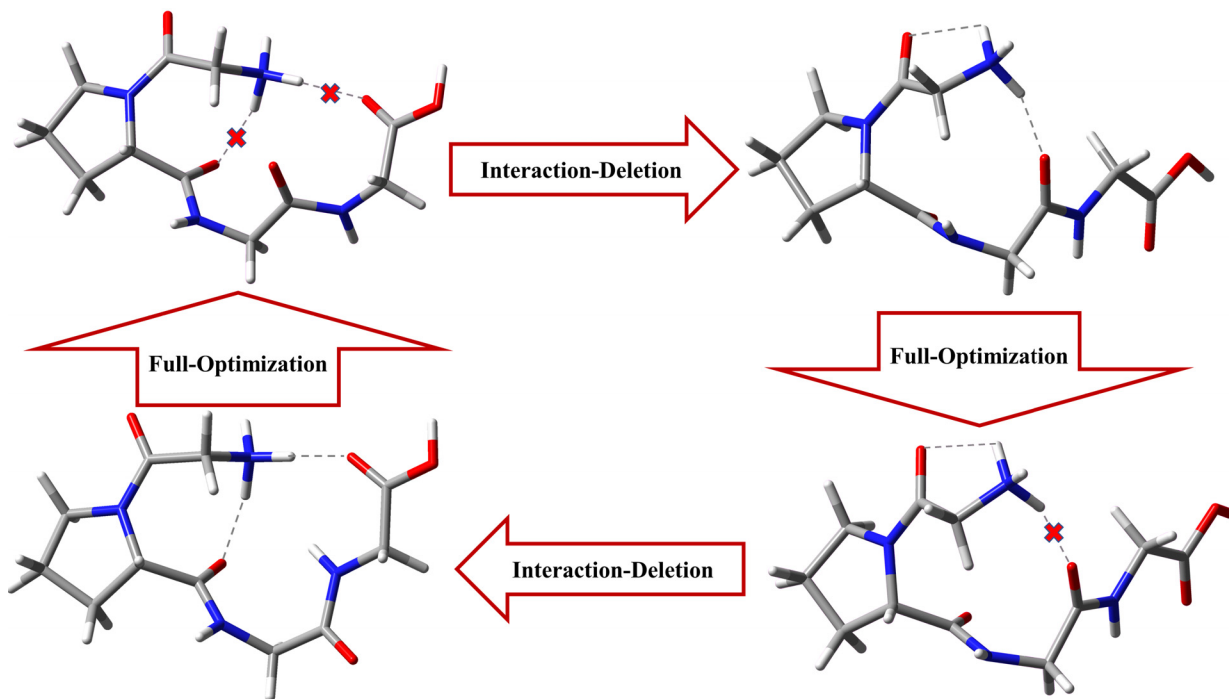


Figure 22. Interaction-deletion cycle for *cis*-c1 H^+GPGG . Two intramolecular hydrogen bonds were deleted in the first step, leading to a new intramolecular hydrogen bond formation between the molecular arms. This newly formed hydrogen bond was deleted in the next step, which restored the two original hydrogen bonds but with a flipped peptide linkage. Full optimization of the resultant conformation in the final step brings it back to its initial conformation. The composite energy scheme for the second interaction-deletion step is depicted in Figure S5.

interactions can be user-defined, and the method is sufficiently general to be used with any ab initio or density functional method. Energies and forces are easily obtained with this composite approach, allowing geometry optimizations that lead to chemically meaningful structures that describe how the removed interactions contribute to the local geometrical minima. We illustrate the application of our new hybrid scheme by computing the influence of intramolecular hydrogen-bonding interactions in two small molecules: 1,6-($\text{tG}^+\text{G}^+\text{TG}^+\text{G}^+\text{g}^-$)-hexanediol and *twist-boat* *cis*-1,4-cyclohexanediol. We demonstrate that the composite method can be extended to larger molecular systems by showing its application on a Si(100) surface model containing interactions between dissociated ammonia and a polypeptide (3_{10} -polyglycine) having multiple intramolecular hydrogen-bonding interactions. Interaction-deletion was also used to explore the nature of hydrogen bond cooperativity in play in 2-nitrobenzene-1,3-diol. Furthermore, we explored hidden conformations of H^+GPGG by switching off its conjoined intramolecular hydrogen-bonding interactions. Therefore, the proposed method is robust and should apply to other complex molecular studies, such as material systems and biomolecules.

■ ASSOCIATED CONTENT

SI Supporting Information

The Supporting Information is available free of charge at <https://pubs.acs.org/doi/10.1021/acs.jpca.1c02918>.

Cartesian coordinates of all the structures (PDF)

■ AUTHOR INFORMATION

Corresponding Author

Krishnan Raghavachari – Department of Chemistry, Indiana University, Bloomington, Indiana 47405, United States;

ORCID: [0000-0003-3275-1426](https://orcid.org/0000-0003-3275-1426); Email: kraghava@indiana.edu

Authors

Ankur K. Gupta – Department of Chemistry, Indiana University, Bloomington, Indiana 47405, United States
Benjamin C. Gamoke – Department of Chemistry, Indiana University, Bloomington, Indiana 47405, United States

Complete contact information is available at:
<https://pubs.acs.org/10.1021/acs.jpca.1c02918>

Notes

The authors declare no competing financial interest.

■ ACKNOWLEDGMENTS

This work was supported by the Chemical Sciences, Geosciences and Biosciences Division, Office of Basic Energy Sciences, Office of Science, U.S. Department of Energy (DEFG02-09ER16068). This research was supported in part by Lilly Endowment, Inc., through its support for the Indiana University Pervasive Technology Institute. We thank Dr. Nicholas J. Mayhall (Department of Chemistry, Virginia Tech, Blacksburg, VA 24060) for useful ideas and scientific discussions.

■ REFERENCES

- (1) Dill, K. A. Dominant forces in protein folding. *Biochemistry* 1990, 29 (31), 7133–7155.
- (2) Dill, K. A.; MacCallum, J. L. The Protein-Folding Problem, 50 Years On. *Science* 2012, 338 (6110), 1042.
- (3) Aparicio, S.; Atilhan, M.; Karadas, F. Thermophysical Properties of Pure Ionic Liquids: Review of Present Situation. *Ind. Eng. Chem. Res.* 2010, 49 (20), 9580–9595.

(4) Marsh, K. N.; Boxall, J. A.; Lichtenthaler, R. Room temperature ionic liquids and their mixtures—a review. *Fluid Phase Equilib.* **2004**, *219* (1), 93–98.

(5) Niedermeyer, H.; Hallett, J. P.; Villar-Garcia, I. J.; Hunt, P. A.; Welton, T. Mixtures of ionic liquids. *Chem. Soc. Rev.* **2012**, *41* (23), 7780–7802.

(6) Ballester, P. Anion binding in covalent and self-assembled molecular capsules. *Chem. Soc. Rev.* **2010**, *39* (10), 3810–3830.

(7) Li, Y.; Pink, M.; Karty, J. A.; Flood, A. H. Dipole-Promoted and Size-Dependent Cooperativity between Pyridyl-Containing Triazolophanes and Halides Leads to Persistent Sandwich Complexes with Iodide. *J. Am. Chem. Soc.* **2008**, *130* (51), 17293–17295.

(8) Srinivasan, A.; Ishizuka, T.; Osuka, A.; Furuta, H. Doubly N-Confused Hexaphyrin: A Novel Aromatic Expanded Porphyrin that Complexes Bis-metals in the Core. *J. Am. Chem. Soc.* **2003**, *125* (4), 878–879.

(9) Chalasinski, G.; Szczesniak, M. M. Origins of Structure and Energetics of van der Waals Clusters from ab Initio Calculations. *Chem. Rev.* **1994**, *94* (7), 1723–1765.

(10) Grabowski, S. J. What Is the Covalency of Hydrogen Bonding? *Chem. Rev.* **2011**, *111* (4), 2597–2625.

(11) Jabłoński, M. *Molecules* **2020**, *25* (23), 5512.

(12) Gonthier, J. F.; Corminboeuf, C. Quantification and Analysis of Intramolecular Interactions. *Chimia* **2014**, *68* (4), 221–226.

(13) Estácio, S. G.; Cabral do Couto, P.; Costa Cabral, B. J.; Minas da Piedade, M. E.; Martinho Simões, J. A. Energetics of Intramolecular Hydrogen Bonding in Di-substituted Benzenes by the ortho–para Method. *J. Phys. Chem. A* **2004**, *108* (49), 10834–10843.

(14) Schuster, P.; Zundel, G.; Sandorfy, C. In *Hydrogen Bond; Recent Developments in Theory and Experiments*; North-Holland Publishing Company: 1976.

(15) Rozas, I.; Alkorta, I.; Elguero, J. Intramolecular Hydrogen Bonds in ortho-Substituted Hydroxybenzenes and in 8-Susbtituted 1-Hydroxynaphthalenes: Can a Methyl Group Be an Acceptor of Hydrogen Bonds? *J. Phys. Chem. A* **2001**, *105* (45), 10462–10467.

(16) Wheeler, S. E.; Houk, K. N.; Schleyer, P. v. R.; Allen, W. D. A Hierarchy of Homodesmotic Reactions for Thermochemistry. *J. Am. Chem. Soc.* **2009**, *131* (7), 2547–2560.

(17) Buemi, G.; Zuccarello, F. Is the intramolecular hydrogen bond energy valuable from internal rotation barriers? *J. Mol. Struct.: THEOCHEM* **2002**, *581* (1), 71–85.

(18) Nowroozi, A.; Hajiabadi, H.; Akbari, F. OH···O and OH···S intramolecular interactions in simple resonance-assisted hydrogen bond systems: a comparative study of various models. *Struct. Chem.* **2014**, *25* (1), 251–258.

(19) Nowroozi, A.; Raissi, H.; Farzad, F. The presentation of an approach for estimating the intramolecular hydrogen bond strength in conformational study of β -Aminoacrolein. *J. Mol. Struct.: THEOCHEM* **2005**, *730* (1), 161–169.

(20) Rusinska-Roszak, D.; Sowinski, G. Estimation of the Intramolecular O–H···O=C Hydrogen Bond Energy via the Molecular Tailoring Approach. Part I: Aliphatic Structures. *J. Chem. Inf. Model.* **2014**, *54* (7), 1963–1977.

(21) Gadre, S. R.; Shirsat, R. N.; Limaye, A. C. Molecular Tailoring Approach for Simulation of Electrostatic Properties. *J. Phys. Chem.* **1994**, *98* (37), 9165–9169.

(22) Deshmukh, M. M.; Gadre, S. R.; Bartolotti, L. J. Estimation of Intramolecular Hydrogen Bond Energy via Molecular Tailoring Approach. *J. Phys. Chem. A* **2006**, *110* (45), 12519–12523.

(23) Deshmukh, M. M.; Suresh, C. H.; Gadre, S. R. Intramolecular Hydrogen Bond Energy in Polyhydroxy Systems: A Critical Comparison of Molecular Tailoring and Isodesmic Approaches. *J. Phys. Chem. A* **2007**, *111* (28), 6472–6480.

(24) Deshmukh, M. M.; Bartolotti, L. J.; Gadre, S. R. Intramolecular Hydrogen Bonding and Cooperative Interactions in Carbohydrates via the Molecular Tailoring Approach. *J. Phys. Chem. A* **2008**, *112* (2), 312–321.

(25) Deshmukh, M. M.; Gadre, S. R. Estimation of N–H···O=C Intramolecular Hydrogen Bond Energy in Polypeptides. *J. Phys. Chem. A* **2009**, *113* (27), 7927–7932.

(26) Su, P.; Chen, Z.; Wu, W. An energy decomposition analysis study for intramolecular non-covalent interaction. *Chem. Phys. Lett.* **2015**, *635*, 250–256.

(27) Gonthier, J. F.; Corminboeuf, C. Exploration of zeroth-order wavefunctions and energies as a first step toward intramolecular symmetry-adapted perturbation theory. *J. Chem. Phys.* **2014**, *140* (15), 154107.

(28) Parrish, R. M.; Gonthier, J. F.; Corminboeuf, C.; Sherrill, C. D. Communication: Practical intramolecular symmetry adapted perturbation theory via Hartree-Fock embedding. *J. Chem. Phys.* **2015**, *143* (5), 051103.

(29) Pastorczak, E.; Prlj, A.; Gonthier, J. F.; Corminboeuf, C. Intramolecular symmetry-adapted perturbation theory with a single-determinant wavefunction. *J. Chem. Phys.* **2015**, *143* (22), 224107.

(30) Patkowski, K. Recent developments in symmetry-adapted perturbation theory. *Wiley Interdiscip. Rev.: Comput. Mol. Sci.* **2020**, *10* (3), e1452.

(31) Weinhold, F.; Landis, C. R.; Press, C. U. *Valency and Bonding: A Natural Bond Orbital Donor-Acceptor Perspective*; Cambridge University Press: 2005.

(32) Szatylowicz, H.; Jeziorska, A.; Sadlej-Sosnowska, N. Correlations of NBO energies of individual hydrogen bonds in nucleic acid base pairs with some QTAIM parameters. *Struct. Chem.* **2016**, *27* (1), 367–376.

(33) Szatylowicz, H.; Sadlej-Sosnowska, N. Characterizing the Strength of Individual Hydrogen Bonds in DNA Base Pairs. *J. Chem. Inf. Model.* **2010**, *50* (12), 2151–2161.

(34) Johnson, E. R.; Keinan, S.; Mori-Sánchez, P.; Contreras-García, J.; Cohen, A. J.; Yang, W. Revealing Noncovalent Interactions. *J. Am. Chem. Soc.* **2010**, *132* (18), 6498–6506.

(35) Contreras-García, J.; Johnson, E. R.; Keinan, S.; Chaudret, R.; Piquemal, J.-P.; Beratan, D. N.; Yang, W. NCIPILOT: A Program for Plotting Noncovalent Interaction Regions. *J. Chem. Theory Comput.* **2011**, *7* (3), 625–632.

(36) Bader, R. F. W. Atoms in molecules. *Acc. Chem. Res.* **1985**, *18* (1), 9–15.

(37) Bader, R. F. W. A quantum theory of molecular structure and its applications. *Chem. Rev.* **1991**, *91* (5), 893–928.

(38) Becke, A. D.; Edgecombe, K. E. A simple measure of electron localization in atomic and molecular systems. *J. Chem. Phys.* **1990**, *92* (9), 5397–5403.

(39) Silvi, B.; Savin, A. Classification of chemical bonds based on topological analysis of electron localization functions. *Nature* **1994**, *371* (6499), 683–686.

(40) Guevara-Vela, J. M.; Romero-Montalvo, E.; Mora Gómez, V. A.; Chávez-Calvillo, R.; García-Revilla, M.; Francisco, E.; Pendás, Á. M.; Rocha-Rinza, T. Hydrogen bond cooperativity and anticooperativity within the water hexamer. *Phys. Chem. Chem. Phys.* **2016**, *18* (29), 19557–19566.

(41) Nochebuena, J.; Cuautli, C.; Ireta, J. Origin of cooperativity in hydrogen bonding. *Phys. Chem. Chem. Phys.* **2017**, *19* (23), 15256–15263.

(42) Dapprich, S.; Komáromi, I.; Byun, K. S.; Morokuma, K.; Frisch, M. J. A new ONIOM implementation in Gaussian98. Part I. The calculation of energies, gradients, vibrational frequencies and electric field derivatives¹Dedicated to Professor Keiji Morokuma in celebration of his 65th birthday. *J. Mol. Struct.: THEOCHEM* **1999**, *461*–462, 1–21.

(43) Chung, L. W.; Sameera, W. M. C.; Ramozzi, R.; Page, A. J.; Hatanaka, M.; Petrova, G. P.; Harris, T. V.; Li, X.; Ke, Z.; Liu, F.; et al. The ONIOM Method and Its Applications. *Chem. Rev.* **2015**, *115* (12), 5678–5796.

(44) Jose, K. V. J.; Raghavachari, K. Evaluation of Energy Gradients and Infrared Vibrational Spectra through Molecules-in-Molecules Fragment-Based Approach. *J. Chem. Theory Comput.* **2015**, *11* (3), 950–961.

(45) Chen, H.-Y.; Cheng, Y.-L.; Takahashi, K. Theoretical Calculation of the OH Vibrational Overtone Spectra of 1,5-Pentanediol and 1,6-Hexanediol. *J. Phys. Chem. A* **2011**, *115* (50), 14315–14324.

(46) Møller, C.; Plesset, M. S. Note on an Approximation Treatment for Many-Electron Systems. *Phys. Rev.* **1934**, *46* (7), 618–622.

(47) Dunning, T. H. Gaussian basis sets for use in correlated molecular calculations. I. The atoms boron through neon and hydrogen. *J. Chem. Phys.* **1989**, *90* (2), 1007–1023.

(48) Kendall, R. A.; Dunning, T. H.; Harrison, R. J. Electron affinities of the first-row atoms revisited. Systematic basis sets and wave functions. *J. Chem. Phys.* **1992**, *96* (9), 6796–6806.

(49) Zhao, Y.; Truhlar, D. G. The M06 suite of density functionals for main group thermochemistry, thermochemical kinetics, non-covalent interactions, excited states, and transition elements: two new functionals and systematic testing of four M06-class functionals and 12 other functionals. *Theor. Chem. Acc.* **2008**, *120* (1), 215–241.

(50) Grimme, S.; Antony, J.; Ehrlich, S.; Krieg, H. A consistent and accurate ab initio parametrization of density functional dispersion correction (DFT-D) for the 94 elements H–Pu. *J. Chem. Phys.* **2010**, *132* (15), 154104.

(51) Grimme, S.; Ehrlich, S.; Goerigk, L. Effect of the damping function in dispersion corrected density functional theory. *J. Comput. Chem.* **2011**, *32* (7), 1456–1465.

(52) Becke, A. D. Density-functional thermochemistry. I. The effect of the exchange-only gradient correction. *J. Chem. Phys.* **1992**, *96* (3), 2155–2160.

(53) Lee, C.; Yang, W.; Parr, R. G. Development of the Colle-Salvetti correlation-energy formula into a functional of the electron density. *Phys. Rev. B: Condens. Matter Mater. Phys.* **1988**, *37* (2), 785–789.

(54) Becke, A. D. Density-functional thermochemistry. V. Systematic optimization of exchange-correlation functionals. *J. Chem. Phys.* **1997**, *107* (20), 8554–8560.

(55) Schmider, H. L.; Becke, A. D. Optimized density functionals from the extended G2 test set. *J. Chem. Phys.* **1998**, *108* (23), 9624–9631.

(56) Chai, J.-D.; Head-Gordon, M. Long-range corrected hybrid density functionals with damped atom–atom dispersion corrections. *Phys. Chem. Chem. Phys.* **2008**, *10* (44), 6615–6620.

(57) Allerhand, A.; Von Rague Schleyer, P. A Survey of C–H Groups as Proton Donors in Hydrogen Bonding. *J. Am. Chem. Soc.* **1963**, *85* (12), 1715–1723.

(58) McDowell, S. A. C.; Buckingham, A. D. On the Correlation between Bond-Length Change and Vibrational Frequency Shift in Hydrogen-Bonded Complexes: A Computational Study of Y–HCl Dimers (Y = N₂, CO, BF). *J. Am. Chem. Soc.* **2005**, *127* (44), 15515–15520.

(59) Frisch, M. J.; Trucks, G. W.; Schlegel, H. B.; Scuseria, G. E.; Robb, M. A.; Cheeseman, J. R.; Scalmani, G.; Barone, V.; Petersson, G. A.; Nakatsuji, H.; et al. *Gaussian 16, Rev. C.01*; Wallingford, CT, 2016.

(60) Stolow, R. D. Intramolecular Hydrogen Bonding in Non-Chair Conformations of cis-1,4-cyclohexanediols. *J. Am. Chem. Soc.* **1961**, *83* (11), 2592–2593.

(61) Shikata, T.; Okuzono, M. Hydration/Dehydration Behavior of Polyalcoholic Compounds Governed by Development of Intramolecular Hydrogen Bonds. *J. Phys. Chem. B* **2013**, *117* (9), 2782–2788.

(62) Kaupp, M.; Metz, B.; Stoll, H. Breakdown of Bond Length–Bond Strength Correlation: A Case Study. *Angew. Chem., Int. Ed.* **2000**, *39* (24), 4607–4609.

(63) Kaupp, M.; Danovich, D.; Shaik, S. Chemistry is about energy and its changes: A critique of bond-length/bond-strength correlations. *Coord. Chem. Rev.* **2017**, *344*, 355–362.

(64) Dixon, D. A.; Komornicki, A. Ab initio conformational analysis of cyclohexane. *J. Phys. Chem.* **1990**, *94* (14), 5630–5636.

(65) Gamoke, B. C.; Mayhall, N. J.; Raghavachari, K. A Composite Energy Treatment for Sterically Hindered Cluster Models for the Si(100) Surface. *J. Chem. Theory Comput.* **2012**, *8* (12), 5132–5136.

(66) Gamoke, B. C.; Mayhall, N. J.; Raghavachari, K. Modeling Nonperiodic Adsorption on Periodic Surfaces: A Composite Energy Approach for Low-Coverage Limits. *J. Phys. Chem. C* **2012**, *116* (22), 12048–12054.

(67) Queeney, K. T.; Chabal, Y. J.; Raghavachari, K. Role of Interdimer Interactions in NH₃ Dissociation on Si(100)-(2 × 1). *Phys. Rev. Lett.* **2001**, *86* (6), 1046–1049.

(68) Bischoff, J. L.; Kubler, L.; Bolmont, D.; Sébenne, C. A.; Lacharme, J. P.; Bonnet, J. E.; Hricovini, K. A photoemission study of ammonia adsorption on Si(100)2 × 1 and Si(111)2 × 1 surfaces. *Surf. Sci.* **1993**, *293* (1), 35–40.

(69) Hlil, E. K.; Kubler, L.; Bischoff, J. L.; Bolmont, D. Photoemission study of ammonia dissociation on Si(100) below 700 K. *Phys. Rev. B: Condens. Matter Mater. Phys.* **1987**, *35* (11), 5913–5916.

(70) Smedarchina, Z.; Zgierski, M. Model, First-Principle Calculation of Ammonia Dissociation on Si(100) Surface. Importance of Proton Tunneling. *Int. J. Mol. Sci.* **2003**, *4* (7), 445.

(71) Widjaja, Y.; Mysinger, M. M.; Musgrave, C. B. Ab Initio Study of Adsorption and Decomposition of NH₃ on Si(100)-(2 × 1). *J. Phys. Chem. B* **2000**, *104* (11), 2527–2533.

(72) Beckett, D.; El-Baba, T. J.; Clemmer, D. E.; Raghavachari, K. Electronic Energies Are Not Enough: An Ion Mobility-Aided, Quantum Chemical Benchmark Analysis of H(+)GPGG Conformers. *J. Chem. Theory Comput.* **2018**, *14* (10), 5406–5418.